ONLINE FIRST

This is a provisional PDF only. Copyedited and fully formatted versión will be made available at final publication

HISTOLOGY AND HISTOPATHOLOGY

ISSN: 0213-3911
e-ISSN: 1699-5848

Establishment of human acute monocytic leukemia model with systemic infiltration in NPG mice

Authors: Jing Xu, Qiong Wu, Yanfei Rao, Zhenjiang Li, Wenfeng He, Wanlei Sun, Jifu Zheng, Qingming Wang and Aiping Tang

DOI: 10.14670/HH-18-742
Article type: ORIGINAL ARTICLE
Accepted: 2024-04-04
Epub ahead of print: 2024-04-04

Establishment of human acute monocytic leukemia model with systemic infiltration in NPG mice

Jing Xu[1], Qiong Wu[2], Yanfei Rao[2], Zhenjiang Li[1*], Wenfeng He[3], Wanlei Sun[2], Jifu Zheng[1], Qingming Wang[1], Aiping Tang[1]

Running title: a systemic leukemia model in NPG mice

[1] Department of Hematology, The Second Affiliated Hospital of Nanchang University, Nanchang, China

[2] Department of Clinical Laboratory, The Second Affiliated Hospital of Nanchang University, Nanchang, China

[3] Key laboratory of molecular medicine of Jiangxi, The second affiliated hospital of Nanchang university, Nanchang, China

*Correspondence: Zhenjiang Li, PHD, Associate professor, Department of Hematology, The Second Affiliated Hospital of Nanchang University, No. 1 Minde Road, Donghu District, Nanchang 330006, Jiangxi, China. Phone: 0086-0791-86300483 Email: lzjdgh@163.com.

Abstract. A model construction of systemic acute leukemia is challenging. Herein, we established a systemic leukemia mouse model using highly immunodeficient NPG mice without any immunosuppressive treatments. NPG mice received tail intravenous injection of SHI-1 cells at the concentration of 1×10^7 cells (group A) or 5×10^7 cells (group B) and randomly sacrificed each seven days post-inoculation. Tumor development was monitored using nested-PCR, peripheral blood-smear analysis, flow

cytometry, pathological examinations, and immunohistochemistry. The median survival of mice in groups A and B were 33.0 and 30.0 days, respectively. Blast cells in peripheral blood appeared on day 14 in group B, and on day 21 in group A. In addition, SHI-1 cell specific MLL-AF6 mRNA was detected in both spleen and bone marrow on day 14 post-inoculation. 21 days after inoculation, we observed human $CD45^{+}CD33^{+}$ cells with an SH-1-immunophenotype in the peripheral blood, spleen, and bone marrow, as well as solid neoplasms in multiple organs. Moreover, the histologically infiltrated leukemic cells expressed CD45. In conclusion, the current study demonstrated the normal growth of SHI-1 cells in the NPG mice without immunosuppression, which caused systemic leukemia similar to that observed in acute leukemia patients. We developed an efficient and reproducible model to study leukemia pathogenesis and progression.

Key words: Leukemia animal model, NPG mice, SHI-1 cells, multiple organ infiltration

1. Introduction

Leukemia cells originate from bone marrow and infiltrate into peripheral blood, spleen, liver, lymph nodes, gums, central nervous system (CNS), and other organs (Domingo-Domenech et al., 2000; Stefanidakis et al., 2009). Acute myeloid leukemia (AML) is a malignant disease of myeloid cells in the bone marrow characterized by the increase and mature arrest of myeloid cells, leading to hematopoietic insufficiency. Immunodeficient mice, such as nude mice and NOD-SCID mice, have low counts of functional T and B cells, thereby enabling the fast growth of transplanted cancer cells into solid tumors, thus providing excellent models for various cancers (Flatmark et al., 2004; Chai et al., 2018; Pillai et al., 2018). However, the nude and NOD-SCID mice have residual

immune activity cells that pose a challenge for transplanted leukemic cells to grow, unless they are eradicated by irradiation or chemotherapy (Bosma et al., 1983; Marques da Costa et al., 2018). Although mice were pretreated by splenectomy, immunosuppressant or whole-body irradiation, the rate of leukemic cells infiltrated into bone marrow is low (Li et al., 2006). Therefore, it is of great important to establish an appropriate animal model to study human AML.

NOD-SCID gamma (NSG) mouse (NOD.Cg-Prkdcscid II/L2rgtm1vst/vst) is a type of severely immunodeficient mouse that do not express interleukin-2 receptor (IL-2R) gamma chain (IL-2R γc or CD132) (Ishikawa et al., 2005). The gamma chain of IL-2R is a cytokine receptor subunit common to six different IL receptors: IL-2, IL-4, IL-7, IL-9, IL-15, and IL-21. The absence of the IL-2R γc severely compromises the immune functions of the affected mice, and the activity of NK cells is almost completely lost (Shultz et al., 2005). Therefore, NSG mice are suitable for the development of a leukemia model with systemic infiltration, and may be useful to study the disease pathogenesis, and screen therapeutic agents. The NSG mice developed by Vitalstar Biotechnology (Beijing, China) are named as NPG mice, which have an identical genetic background as that of NSG mice (Xu et al., 2015). Here, we hypothesized that a model of human leukemia with systemic infiltration in NPG mice can be constructed by tail intravenous injection of SHI-1 cells. NPG mice received tail intravenous injection of SHI-1 cells at the concentration of 1×10^7 cells or 5×10^7 cells, and the results confirmed our hypothesis, which provides a simple, rapid, and reproducible method for the investigation of leukemia.

2. Materials and methods

2.1 Acute monocytic leukemia cells

The SHI-1 cell line, derived from a patient with refractory acute monocytic leukemia, was kindly provided by Prof. Suning Chen, Institute of Hematology, Jiangsu Province. The SHI-1 cell is a highly tumorigenic human monocytic leukemia cell line characterized with t(6; 11) (q27; q23), MLL-AF6 fusion gene, and p53 gene mutation, which are beneficial for later detection and verification (Chen et al., 2005). The cells were cultured in Iscove's Modified Dulbecco's Medium (Gibco, USA) supplemented with 10% fetal bovine serum (Wisent, AUS) and maintained at 37°C with 5% CO_2 in a humidified atmosphere. Cells in the logarithmic growth phase were inoculated into the NPG mice.

2.2 Animals and experiments

A total of 17 five-week-old male NPG mice were purchased from Vitalstar Biotechnology (Beijing, China), and maintained under specific pathogen-free conditions. After 4 days of adaptive feeding, the mice were randomly divided into two groups: mice in group A (n=7) received tail intravenous injection of SHI-1 cells at the concentration of 1×10^7 cells and mice in group B (n=10) were inoculated with 5×10^7 SHI-1 cells. The concentration of 1×10^7 cells was selected as our previous study (Li et al., 2006). To ensure the success of model construction, we selected a higher number of cells (5×10^7) for the second group to compare the homing sequence of leukemia cells and the effects of different cell amounts. Thereafter, one mouse from each group was sacrificed and autopsied on day 14, 21, and 28, respectively. 0.5 ml of blood was drawn from each mouse at each time point. The animal health and behaviour were monitored every day and the remaining mice were dissected immediately after they were found to

show food avoidance and lethargy. The mice were euthanized with CO_2 inhalation using a gradual-fill method to relieve pain, and CO_2 flow was maintained for at least 1 minute after respiratory arrest to ensure death. Death was identified as the absence of heartbeat and breathing. We confirmed the infiltrative growth of SHI-1 throughout NPG mice by flow cytometry, PCR, and pathological immunohistochemistry as described following, and the success rate was 100%. The animal study was approved by the Ethics Committee of Nanchang Royo Biotech Co,. Ltd (Approval number: RYE2018010401), and all methods were followed in accordance with the approved guidelines including the use of SHI-1 cells at the concentration of 1×10^7 cells and 5×10^7 cells.

2.3 Identification of immature monocytes

Peripheral blood was drawn from the tail-vein each seven days (day 14, 21, and 28) post-inoculation. The obtained blood was smeared on glass slides for Wright's staining, and observed under a light microscope.

2.4 Real time-PCR

The bone marrow, brain, heart, kidneys, liver, spleen, and stomach, were harvested from the dissected mice, and homogenized in TRIzol reagent (Invitrogen, USA) at 4°C. Total RNA was isolated according to the manufacturer's instructions and reverse transcribed into cDNA using M-MLV reverse transcriptase (Takara, JP). The MLL-AF6 fusion gene was amplified by nested-PCR using the primers listed in Table 1 on a GeneAmp PCR System 9600 (ABI, USA). The PCR steps were as follows: initial denaturation of 5 min at 95°C, 30 cycles of 95°C for 30 s, 60°C for 30 s and 72°C for 30 s, and a final elongation at 72°C. The amplified products (fragment length 280 bp) were analyzed by 1.5% agarose gel electrophoresis.

2.5 Flow cytometry

The peripheral blood and the bone marrow were collected from the mandibular region and femur, respectively. The spleen was resected and ground to collect the single cells. All the samples were filtered through a 400 nm mesh and stained in the dark using CD45-percp and CD33-APC antibodies for 15 min at room temperature. In addition, the spleen cells were stained for 15 min with CD45-percp, CD33-APC, CD34-APC, CD117-PE, CD11b-APC, MPO-FITC, CD64-PE, CD15-FITC, CD14-FITC, and CD13-PE antibodies (BD Biosciences, MD, USA) in the dark at room temperature. After washing with cold PBS, the samples were analyzed using a FACScalibur (BD Biosciences, MD, USA). Data were analyzed using CellQuest software (BD Biosciences, MD, USA).

2.6 Histology

The mice were sacrificed on days 14, 21, and 28 after SHI-1 cell inoculation. Autopsies were carefully carried out to identify neoplasms in various tissues. The femur, heart, kidneys, liver, lung, spleen, stomach, testes, head, and spine were collected and fixed in 4% buffered formalin. The femur, head and spine were decalcified in 10% hydrochloric acid for 24h. The head and spine were sectioned as described before (Li et al., 2006). The tissues were then embedded in paraffin, sectioned, and stained with hematoxylin and eosin (H&E). Human-specific anti-CD45 (Servicebio, CHN) and anti-MPO (Servicebio, CHN) monoclonal antibodies were used for immunohistochemistry, and positive staining was detected using 3, 3′-diaminobenzidine - peroxidase (Servicebio, CHN).

Statistical analysis. The data were analyzed using Student's *t*-test and SPSS 20 software (IBM). Differences with the *p*-value <0.05 were considered as statistically significant.

3 Results

3.1 Clinical course

About 21 days after SHI-1 cell inoculation, the mice showed hunched posture and lethargy. The median survival time in group A was 33 days (range, 31-34), which was significantly longer than that in group B (median: 30 days, range 29-31, $p<0.01$).

3.2 Blast cells in peripheral blood

After 14 days of inoculation, Wright's staining showed a few blast cells (pointed by black arrow) in the blood-smear of mice in group B. However, more blast cells were observed in the peripheral blood obtained from the mice in both group A and B on 21 days after inoculation (Fig. 1A).

3.3 Detection of MLL-AF6 fusion gene

The MLL-AF6 fusion gene is specifically expressed in the SHI-1 cells and can be used to identify SHI-1 cell infiltration. On day 14 after inoculation, the MLL-AF6 fusion gene was detected in the spleen of mice in group A, but in the spleen and bone marrow of mice in group B. On day 21, the MLL-AF6 fusion gene could be amplified in the bone marrow, brain, heart, kidneys, liver, spleen, and stomach in both groups (Fig. 1B).

3.4 Flow cytometry

Flow cytometry was performed to distinguish SHI-1 cells and evaluate the immunophenotype of the blast cells in mice. CD45 is a surface marker of leukocytes

(Wang et al., 2023), whereas CD33 is a surface marker of monocytes (Abuaf et al., 2008). $CD45^+CD33^+$ double positive can be used to identify AML cells (Yang et al., 2022). Currently, Targeting CD33 or CD45 is exploited for immunotherapy of AML (Walter et al., 2008; Willier et al., 2021). Thus, $CD45^+CD33^+$ cells were considered as AML cells in mice. On day 21 after inoculation, the percentage of $CD45^+CD33^+$ cells in the peripheral blood of animals in group A and B was 5.16% and 0.82%, respectively. However, on day 28 after inoculation, the percentage of blast cells in peripheral blood, bone marrow, and spleen of the mice was 9.6%, 11.4% and 23.2%, in group A, and 11%, 37.8%, and 60.5% in group B, respectively (Fig. 2A). The percentage of $CD45^+CD33^+$ cells were increased in peripheral blood, bone marrow, and spleen in both A and B groups in a time-dependent manner, which increased to 39.85±4.17%, 42.88±3.31%, and 53.85±3.58% in group A, while it increased to 50.80±3.97%, 52.66±2.57%, and 64.84±5.68% in group B, respectively, in the mice that died naturally (Fig. 2B and Fig. S1). The last mice in group A and group B died naturally on day 34 and 31 after inoculation, respectively. It was worth noting that the proportion of $CD45^+CD33^+$ cells in the peripheral blood, bone marrow, and spleen of animals in group B was significantly higher than that in group A ($p<0.05$).

Since that the SHI-1 cells cultured *in vitro* expressed CD11b, CD13, CD64, CD33 and CD15, and weakly express CD117 and MPO, we used them to identify SHI-1 cells isolated from the spleen in NPG mice. Our results showed that the $CD45^+CD33^+$ cells showed the same immunophenotype as the SHI-1 cells cultured *in vitro* (Fig. 2C).

3.5 Histologic examination

On day 14 after inoculation, neoplasms were observed on the surface of kidney in the group B mice but not in the group A mice, and the weight of spleen in mice of group B

(188.8 mg) was significantly higher than that in group A (47.5 mg) (Fig. 3A). On day 28 post inoculation, neoplasms were observed on the kidneys, spine, spleen, stomach, and the thoracic vertebrae in the animal of group B (Fig. 3B); However, in the animal of group A, neoplasms were only observed in the kidneys, spleen, and stomach. From day 28 after inoculation, mice in both groups began to die because of leukemia, and more neoplasms were found in group B animals. Mice that survived more than 30 days showed green tumors in the lymph nodes of the neck and armpits, heart, peritoneum, mesentery and bladder (Fig. 3C). When the mice were dead, the spleen weight of group A mice was also significantly lower than that of group B ($p<0.05$) (Fig. 3D).

H&E staining of pathological sections showed a few leukemia cells infiltrated in the spleen of mice in both groups on day 14 after inoculation. On day 21, leukemia cells were observed in the heart, kidneys, liver, lung, spleen and stomach of animals in both groups, and the grade of infiltration in the group B animals was more severe than that in group A. 28 days after inoculation, the grade of infiltration was aggravated in both groups (Fig. 4A). For mice that died naturally, leukemia cell infiltration was also found in the brain parenchyma, pia mater, skull, peritoneum, mesentery, and bladder (data not shown). The results of immunohistochemistry showed that the infiltrating cells were strongly positive for $CD45^+$ (Fig. 4B).

4 Discussion

Animal models are valuable tools for studying the pathophysiology and progression of human diseases. Immunodeficient mice, such as nude mice and NOD-SCID mice, have a residual immune system, which poses a challenge for the development of reliable animal modes of AML. Despite the absence of T cell immune function, a few functional B cells and NK cells are retained in nude mice. NK cells exhibit potent cytotoxicity

against leukemia cells, thus most leukemia cell lines can only form subcutaneous xenografts, but not systemic infiltration in nude mice. An in vivo infiltration model in nude mice by tail-vein inoculation requires pretreatment such as splenectomy, radiation, and chemotherapy (Cavallo et al., 1992; Li et al., 2008, 2011). NOD-SCID mice show more severe immunodeficiency than nude mice as they lack almost all of the functional T and B cells, and have significantly reduced NK cell activity. However, the development of a systemic infiltration model using NOD-SCID mice still requires pretreatment with sublethal irradiation (Pearce et al., 2006). Additionally, the NOD-SCID mice have a relatively short lifespan and tend to develop thymoma spontaneously, which may interfere the progression of leukemia (Shultz et al., 1995; Zheng et al., 2015). Previous studies have successfully established a CNS infiltration model of AML by direct inoculation of SHI-1 cells into the cerebral ventricle of NOD-SCID mice without any pretreatment. However, the infiltrated leukemic cells could only be found in the bone marrow and lymph nodes, which were unable to simulate the leukemia pathogenesis faithfully (Li et al., 2014).

NOD-SCID IL2rg (-/-) mice are considered as a suitable model for human cell transplantation due to their high level of immunodeficiency. Moreover, these mice are deficient in innate immunity and show a complete lack of NK cell activity (Puchalapalli et al., 2016; Marques da Costa et al., 2018). Additionally, the NPG mice have a relatively long lifespan and rarely occur immune escape, making them ideal for the establishment of leukemia models (Zhou et al., 2014). Numerous studies have reported the better suitability of the NPG mice to recapitulate the human immune system than NOD/SCID and NOG mice (Shultz et al., 2005; McDermott et al., 2010). In fact, some human cells can only be successfully transplanted in the NPG mice (Agliano et al., 2008). Therefore, the NPG mice model is usually a priority selection for establishing a

human leukemia model (Sanchez et al., 2009; Woiterski et al., 2013; Her et al., 2017). However, to establish a patient-derived xenograft model, NPG mice still require sublethal irradiation to deplete T-cells from the primary leukemia cells before inoculation. A previous study has reported that sublethal irradiation of the NSG mice before inoculation with the primary leukemia cells achieved moderate success in establishing the human leukemia model (Sanchez et al., 2009). Woiterski et al. has performed T-depletion on primary AML cells before inoculation, leading to 91% AML samples being successfully transplanted, and on average, 34.5% of CD45+ cells were detected in peripheral blood (Woiterski et al., 2013). Her et al. has performed sublethal irradiation on neonatal NPG mice, and inoculated 7 AML samples into their livers. After 3-4.5 months, only 3 out of 7 AML samples (42.85%) successfully expanded (proportion of blasts cells in peripheral blood > 10%) (Her et al., 2017). In these reports, the success rate of transplantation was approximately 43-90%, and the expansion degree of primary leukemia cells varied widely. Moreover, a lower proportion of AML cells in NSG mice may fail to replicate the clinical manifestations of AML patients.

Herein, we established a better systemic leukemia infiltration model using NPG mice and SHI-1 cell line. The concentration of 1×10^7 cells was selected as in our previous study (Li et al., 2006). To ensure the success of model construction, we selected a higher number of cells (5×10^7) for the second group to compare the homing sequence of leukemia cells and the effects of different cell amounts. To avoid the influence of hormones, we chose male mice as our study subjects. The results demonstrated the absence of blast cells in the peripheral blood of mice in group A 14 days after inoculation, and the expression of MLL-AF6 fusion gene was detected only in the spleen. However, a few blast cells were found in the peripheral blood and the MLL-AF6 fusion gene was observed in the bone marrow and spleen of mice in group B.

This indicated that in the NPG model, SHI-1 cells first harbored to the spleen, then to the bone marrow. 21 days after inoculation, a small number of blast cells were observed in the peripheral blood in both group A and group B. Flow cytometry showed the presence of $CD45^{+}CD33^{+}$ cells in the peripheral blood of mice in both groups. In addition, the MLL-AF6 fusion gene was amplified in the heart, liver, spleen, stomach, and kidneys. The Results of histopathology and immunohistochemistry confirmed the infiltration of leukemia cells in multiple organs. On day 21 after inoculation, the mice began to deteriorate and died spontaneously from day 28. Autopsies revealed leukemia cell infiltration and tumor-like growth in multiple organs including the heart, kidneys, liver, lymph nodes, mesentery, spleen, and stomach. Moreover, the proportion of $CD45^{+}CD33^{+}$ cells in the peripheral blood, bone marrow, and spleen was significantly higher than that on day 21. Immunophenotyping revealed that the $CD45^{+}$ cells in the spleen showed the same phenotype as the SHI-1 cells cultured in vitro, indicating that the SHI-1 cells could maintain their primitive feature in the NPG mice.

Leukemia cell infiltration was observed in the meningeal and spinal cord lumen of mice that died spontaneously, suggesting that leukemia cells eventually invaded the CNS. However, we did not observe any partial hemiplegia or limb paralysis in mice, which might be associated either with the shorter survival time of mice, or with the insufficient degree of leukemia infiltration in the CNS that was not enough to cause neurological symptoms. Expectedly, the overall survival of mice in group B was significantly shorter than that in group A and the degree of leukemia infiltration was significantly higher in group B mice, indicating that the survival of the NPG mice is closely related to the number of inoculated AML cells, and the degree of leukemia cell infiltration.

In summary, our present study developed a reliable animal model to investigate the

mechanism of AML progression, and to screen potential therapeutic drugs for human AML. However, the rapid evolution of the disease seriously limits the study of antitumor treatments or dissemination patterns. We will select a lower cellular concentration in subsequent anti-tumor treatment experiments to complement our current study. In addition, the follow up studies will be designed to investigate the conditions of other AML cells, such as Thp1 and HL60 to construct much more leukemia models in NPG mice.

Acknowledgements: We gratefully thank Prof. Suning Chen for providing the SHI-1 cell line. This paper has been presented as a poster at the American Society of Hematology Annual Meeting held in the United States from December 01, 2018 to December 04, 2018.

Funding information: This study was supported by the National Natural Science Foundation of China (Grant No. 82260037 and 81460029) and Jiangxi "5511" Science and Technology Innovation Talent Project (Grant No. 20171BCB18003).

Author contributions: JX constructed animal models and drafted the manuscript. QW performed the flow cytometry assay. YFR performed the blood smear assay. ZJL designed and implemented the projected. WLS performed the Real time-PCR assay. WFH, JFZ, QMW, and APT directed experiments. All the authors approved the final manuscript.

Conflict of interest: The authors state that there are no conflicts of interest to disclose.

Data availability statement: All data will be made available on reasonable request from corresponding authors

Ethics approval statement: The animal study was approved by the Ethics Committee of Nanchang Royo Biotech Co,. Ltd (Approval number: RYE2018010401), and all methods were followed in accordance with the approved guidelines including the use of SHI-1 cells at the concentration of 1×10^7 cells and 5×10^7 cells.

References

Abuaf N., Rostane H., Rajoely B., Gaouar H., Autegarden J., Leynadier F. and Girot R. (2008). Comparison of two basophil activation markers CD63 and CD203c in the diagnosis of amoxicillin allergy. Clin. Exp. Allergy 38, 921-929.

Agliano A., Martin-Padura I., Mancuso P., Marighetti P., Rabascio C., Pruneri G., Shultz L.D. and Bertolini F. (2008). Human acute leukemia cells injected in NOD/LtSz-scid/IL-2Rgamma null mice generate a faster and more efficient disease compared to other NOD/scid-related strains. Int. J. Cancer 123, 2222-2227.

Bosma G.C., Custer R.P. and Bosma M.J. (1983). A severe combined immunodeficiency mutation in the mouse. Nature. 301, 527-530.

Cavallo F., Forni M., Riccardi C., Soleti A., Di Pierro F. and Forni G. (1992). Growth and spread of human malignant T lymphoblasts in immunosuppressed nude mice: a model for meningeal leukemia. Blood. 80, 1279-1283.

Chai Y., Wang H. and Zhou F. (2018). Establishment and characterization of a cell line HCS1220 from human liver metastasis of colon cancer. Cancer Cell Int. 18, 137.

Chen S., Xue Y., Zhang X., Wu Y., Pan J., Wang Y., and Ceng J. (2005). A new human acute monocytic leukemia cell line SHI-1 with t(6;11)(q27;q23), p53 gene alterations and high tumorigenicity in nude mice. Haematologica 90, 766-775.

Domingo-Domenech E., Boqué C., Narvaez J.A., Romagosa V., Domingo-Claros A. and Granena A. (2000). Acute monocytic leukemia in the adult presenting with associated extramedullary gastric infiltration and ascites. Haematologica 85, 875-877.

Flatmark K., Maelandsmo G.M., Martinsen M., Rasmussen H. and Fodstad O. (2004). Twelve colorectal cancer cell lines exhibit highly variable growth and metastatic capacities in an orthotopic model in nude mice. Eur. J. Cancer 40, 1593-1598.

Her Z., Yong K.S.M., Paramasivam K., Tan W.W.S., Chan X.Y., Tan S.Y., Liu M., Fan Y., Linn Y.C., Hui K.M., Surana U. and Chen Q. (2017). An improved pre-clinical patient-derived liquid xenograft mouse model for acute myeloid leukemia. J. Hematol. Oncol. 10, 162.

Ishikawa F., Yasukawa M., Lyons B., Yoshida S., Miyamoto T., Yoshimoto G., Watanabe T., Akashi K., Shultz L.D. and Harada M. (2005). Development of functional human blood and immune systems in NOD/SCID/IL2 receptor {gamma} chain(null) mice. Blood. 106, 1565-1573.

Li Z., Chen Z., Lu J., Cen J., He J., Chen S., Xue Y. and Guo L. (2006). Establishment of a nude mice model of human monocytic leukemia with CNS and multiorgan extramedullary infiltration. Eur. J. Haematol. 77, 128-133.

Li L.X., Tang Y.M., Gu W.Z., Tang H.F., Qian B.Q., Shen H.Q. and Luo C.F. (2008). Establishment of animal model with B lineage acute leukemia in nude mice for evaluation of new therapeutic agents. Zhejiang Da Xue Xue Bao Yi Xue Ban. 37, 511-514 (in Chinese).

Li X.M., Ding X., Zhang L.Z., Cen J.N. and Chen Z.X. (2011). Preliminary establishment of transplanted human chronic myeloid leukemia model in nude mice. Zhongguo Shi Yan Xue Ye Xue Za Zhi. 19, 1378-1382 (in Chinese).

Li D., Li P., He Z., Meng Z., Luo X. and Fang J. (2014). Establishment of NOD/SCID mouse model of central nervous system leukemia. Oncol. Rep. 32, 684-690.

Marques da Costa M.E., Daudigeos-Dubus E., Gomez-Brouchet A., Bawa O., Rouffiac V., Serra M., Scotlandi K., Santos C., Geoerger B. And Gaspar N. (2018). Establishment and characterization of in vivo orthotopic bioluminescent xenograft models from human osteosarcoma cell lines in Swiss nude and NSG mice. Cancer Med. 7, 665-676.

McDermott S.P., Eppert K., Lechman E.R, Doedens M. and Dick J.E. (2010). Comparison of human cord blood engraftment between immunocompromised mouse strains. Blood. 116, 193-200.

Pearce D.J., Taussig D., Zibara K., Smith L.L., Ridler C.M., Preudhomme C., Young B.D., Rohatiner A.Z., Lister T.A. and Bonnet D. (2006). AML engraftment in the NOD/SCID assay reflects the outcome of AML: implications for our understanding of the heterogeneity of AML. Blood. 107, 1166-1173.

Pillai S.G., Li S., Siddappa C.M., Ellis M.J., Watson M.A., Aft R. (2018). Identifying biomarkers of breast cancer micrometastatic disease in bone marrow using a patient-derived xenograft mouse model. Breast Cancer Res. 20, 2.

Puchalapalli M., Zeng X., Mu L., Anderson A., Hix Glickman L., Zhang M., Sayyad M.R., Wangensteen S.M., Clevenger C.V. and Koblinski J.E. (2016). NSG mice provide a better spontaneous model of breast cancer metastasis than athymic (Nude) mice. PLoS One 11, e0163521.

Sanchez P.V., Perry R.L., Sarry J.E., Perl A.E., Murphy K., Swider C.R., Bagg A., Choi J.K., Biegel J.A., Danet-Desnoyers G. and Carroll M. (2009). A robust xenotransplantation model for acute myeloid leukemia. Leukemia 23, 2109-2117.

Shultz L.D., Schweitzer P.A., Christianson S.W., Gott B., Schweitzer I.B., Tennent B., Mckenna S., Mobraaten L., Rajan T.V., Greiner D.L. and Leiter E.H. (1995). Multiple defects in innate and adaptive immunologic function in NOD/LtSz-*scid* mice. J. Immunol. 154, 180-191.

Shultz L.D., Lyons B.L., Burzenski L.M., Gott B., Chen X., Chaleff S., Kotb M., Gillies S.D., King M., Mangada J., Greiner D.L. and Handgretinger R. (2005). Human lymphoid and myeloid cell development in NOD/LtSz-scid IL2R gamma null mice engrafted with mobilized human hemopoietic stem cells. J. Immunol. 174, 6477-6489.

Stefanidakis M., Karjalainen K., Jaalouk D.E., Gahmberg C.G., O'Brien S., Pasqualini R., Arap W. and Koivunen E. (2009). Role of leukemia cell invadosome in extramedullary infiltration. Blood. 114, 3008-3017.

Walter R., Boyle K., Appelbaum F., Bernstein I. and Pagel J. (2008). Simultaneously targeting CD45 significantly increases cytotoxicity of the anti-CD33 immunoconjugate, gemtuzumab ozogamicin, against acute myeloid leukemia (AML) cells and improves survival of mice bearing human AML xenografts. 111, 4813-4819.

Wang X., Luo J., Wang J., Cao J., Hong Y., Wen Q., Zeng Y., Shi Z., Ma G., Zhang T. Huang P. (2023). Catalytically active Metal-Organic frameworks elicit robust immune response to combination chemodynamic and checkpoint blockade immunotherapy. ACS Appl. Mater. Interfaces. 15, 6442-6455.

Willier S., Rothämel P., Hastreiter M., Wilhelm J., Stenger D., Blaeschke F., Rohlfs M., Kaeuferle T., Schmid I., Albert M.H., Binder V., Subklewe M., Klein C. and Feuchtinger T. (2021). CLEC12A and CD33 coexpression as a preferential target for pediatric AML combinatorial immunotherapy. Blood. 137, 1037-1049.

Woiterski J., Ebinger M., Witte K.E., Goecke B., Heininger V., Philippek M., Bonin M., Schrauder A., Röttgers S., Herr W., Lang P., Handgretinger R., Hartwig U.F. and André M.C. (2013). Engraftment of low numbers of pediatric acute lymphoid and myeloid leukemias into NOD/SCID/IL2Rcγnull mice reflects individual leukemogenecity and highly correlates with clinical outcome. Int. J. Cancer 133,

1547-1556.

Xu Y.R., Li Y.H., Chen S.P., Zou B.H., Zhang Q., Xu M., Kong W.X., Sheng H.X., Hu G.L., Liao L., Zhang B. and Hu L.D. (2015). Establishment of humanized mouse model by using transplantation of mobilized peripheral blood stem cells. Zhongguo Shi Yan Xue Ye Xue Za Zhi. 23, 1753-1757 (in Chinese).

Yang C., Fang Y., Luo X., Teng D., Liu Z., Zhou Y. and Liao G. (2022). Discovery of natural product-like spirooxindole derivatives as highly potent and selective LSD1/KDM1A inhibitors for AML treatment. Bioorg. Chem. 120, 105596.

Zheng Y., Hao S., Hu L. and Cheng T. (2015). Development of immunodeficient mice/humanized mouse models and their applications in hematology research. Zhonghua Xue Ye Xue Za Zhi. 36, 966-971.

Zhou Q., Facciponte J., Jin M., Shen Q. and Lin Q. (2014). Humanized NOD-SCID IL2rg-/- mice as a preclinical model for cancer research and its potential use for individualized cancer therapies. Cancer Lett. 344, 13-19.

Table 1. Primers used for the amplification of MLL-AF6 fusion gene

	Primers	Sequence
First round	Sense	5′-GAGGATCCTGCCCCAAAGAAAAG-3′
	Anti-sense	5′-CTCCGCTGACATGCACTTCATAG-3′
Second round	Sense	5′-TGAGCCCAAGAAAA-AGCAGCCTCCA-3′
	Anti-sense	5′-TACTTGGGAGAG-GACAGCATTCG-3′

Figure legends

Fig 1. Wright's staining and amplification of MLL-AF6 gene.

A. The representative images of Wright's staining on days 14 and 21.

B. Amplification of MLL-AF6 gene. M: Marker; P: SHI-1 Cell; N: normal spleen. lane a1-6: liver, kidney, spleen, stomach, heart and bone marrow of group A mouse on day 14 post-inoculation, lane a7-12: spleen, liver, bone marrow, kidney, stomach and heart of group B mouse on day 14 post-inoculation.

b. B1-7: liver, spleen, kidney, stomach, brain, heart, and bone marrow of group A mouse on day 21 post-inoculation, lane b8-14: liver, heart, kidney, stomach, brain, spleen, and bone marrow of group B mouse on day 21 post-inoculation.

Fig. 2. A: The proportion of $CD45^+CD33^+$ double positive cells in NPG mice on day 28 after inoculation.

The $CD45^+CD33^+$ double positive cells in the peripheral blood, bone marrow and spleen of NPG mice in group A (first line) were less than that of mice in group B (second line) on day 28 post-inoculation.

B: The proportion of $CD45^+CD33^+$ double positive cells in the last dead NPG mice

The $CD45^+CD33^+$ double positive cells in the peripheral blood, bone marrow and spleen of last dead NPG mice in group A were less than that of mice in group B. *$p<0.05$.

C: Immunophenotype of leukemic cells.

The first line shows that SHI-1 cell cultured *in vitro* expressed CD11b, CD13, CD34，CD64, CD33, CD14, CD15, CD117 and MPO. The second line shows the immunophenotype of cells isolated from the spleen of NPG mouse, the CD45+ cells had the same immunophenotype as the human SHI-1 cell cultured in vitro.

Fig. 3. A: The size and the weight of spleen of NPG mice in group A were significantly lower than that in group B. B: SHI-1 cells could grow and form solid neoplasms in the kidneys, liver, spleen, stomach, heart, lymph node and the soft tissues in NPG mice (black arrows) on day 28 post inoculation. C: Mice that survived more than 30 days showed green tumors in the lymph nodes of the neck and armpits, heart, peritoneum, mesentery and bladder. D: Among the mice that died spontaneously, the weight of spleen in group A was significantly lower than that in group B ($p<0.05$).

Fig 4. A: The size and the weight of spleen in the NPG mice sacrificed on day 14, 21 and 28 post-inoculation increased gradually. Meanwhile, the degree of human CD45+ cell infiltration in the spleen was also aggravated in a time dependent manner (brown). B: H&E staining and immunohistochemistry showed that CD45+ leukemic cells infiltrated (black arrow) into the heart, liver, spleen, kidneys, lung, stomach, femur (40×) and spinal cord (10×) of NPG mice inoculated with SHI-1 cells.

Fig. S1 The representative flow cytometry plots of Figure 2B.

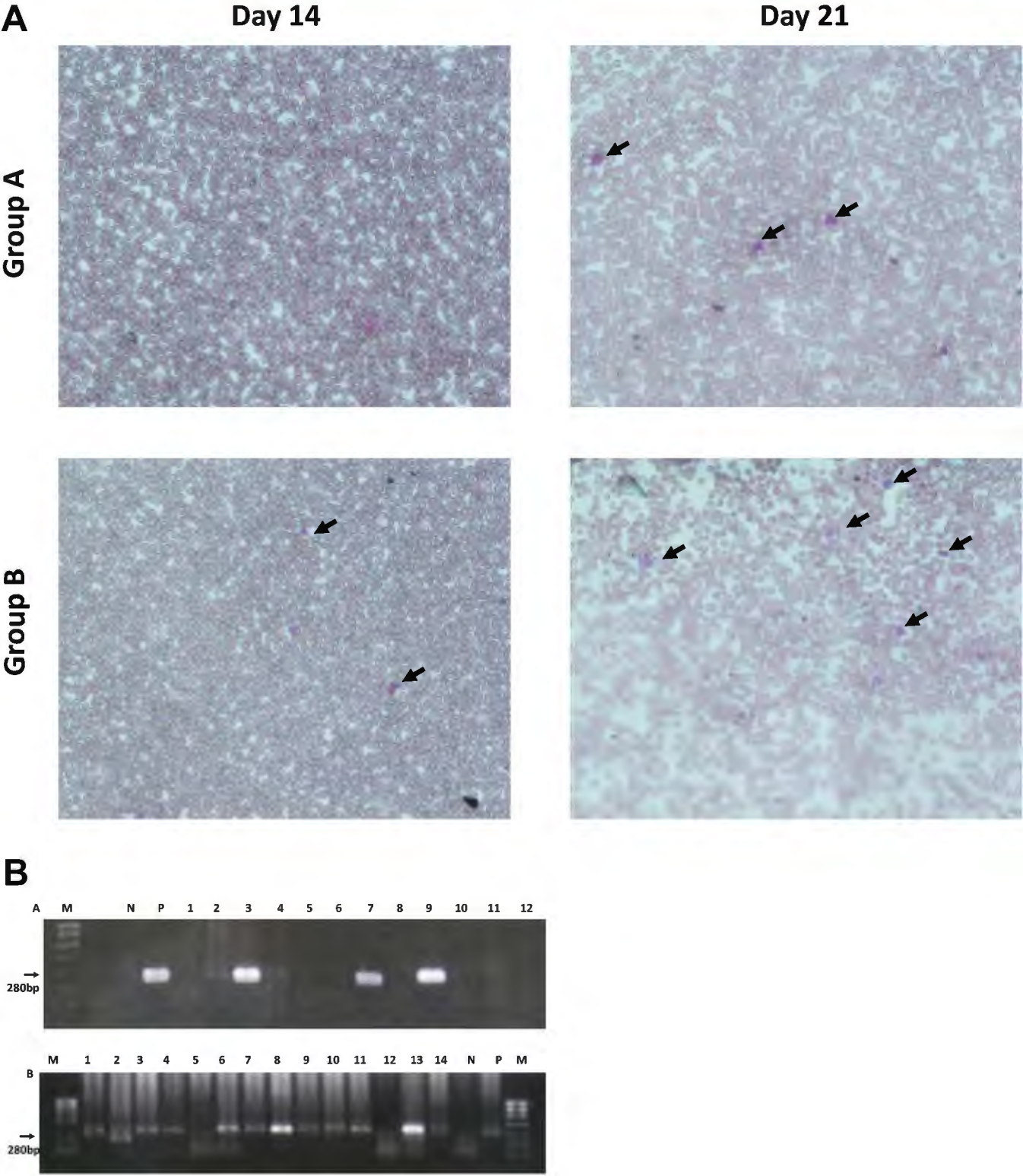
A
Day 14
Day 21
Group A
Group B
B
A M N P 1 2 3 4 5 6 7 8 9 10 11 12
280bp
M 1 2 3 4 5 6 7 8 9 10 11 12 13 14 N P M
B
280bp

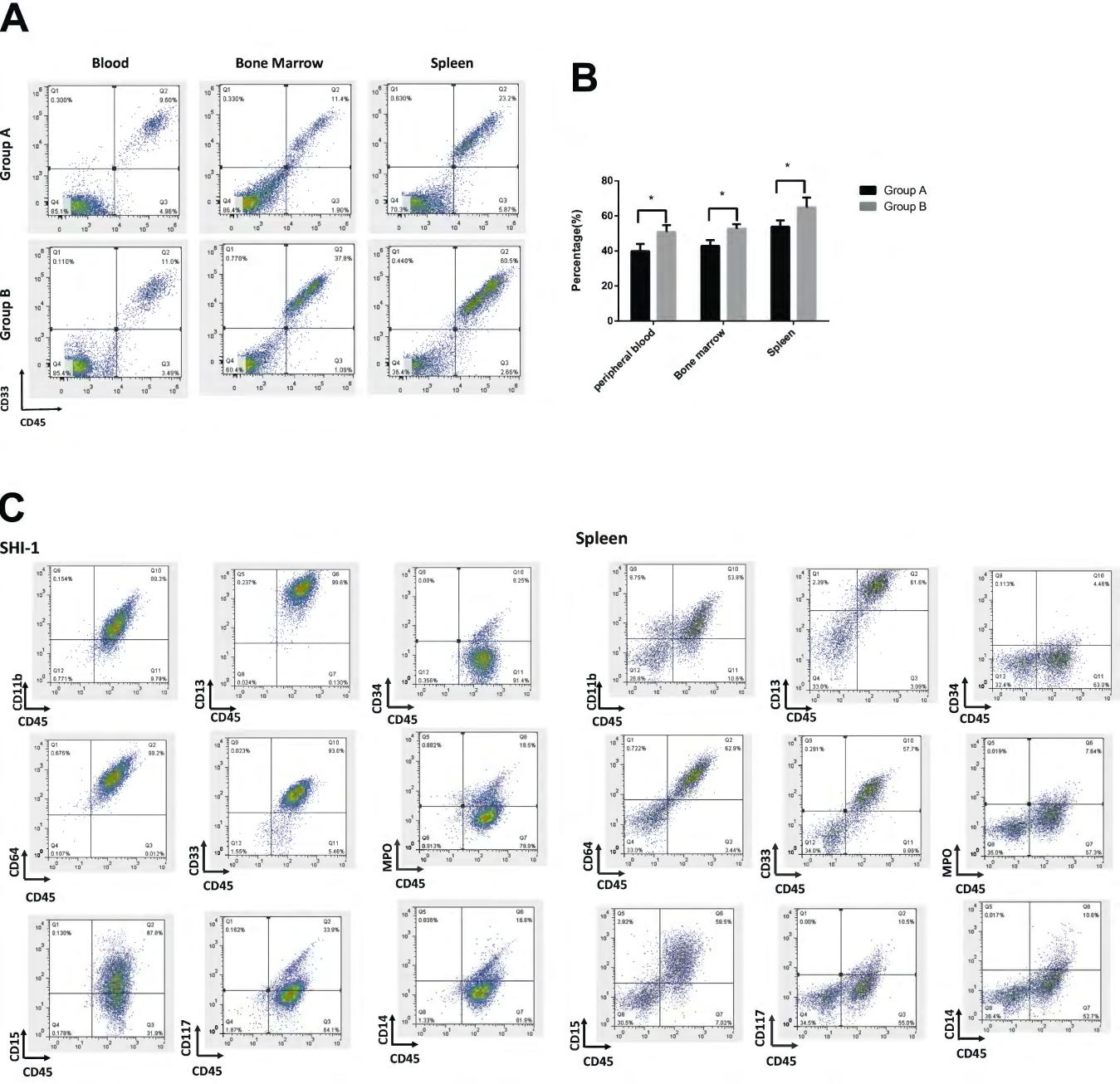
A
Blood
Bone Marrow
Spleen
Group A
Group B
CD33
CD45
B
Percentage(%)
Group A
Group B
peripheral blood
Bone marrow
Spleen
C
SHI-1
Spleen
CD11b
CD13
CD34
CD64
CD33
MPO
CD15
CD117
CD14
CD45

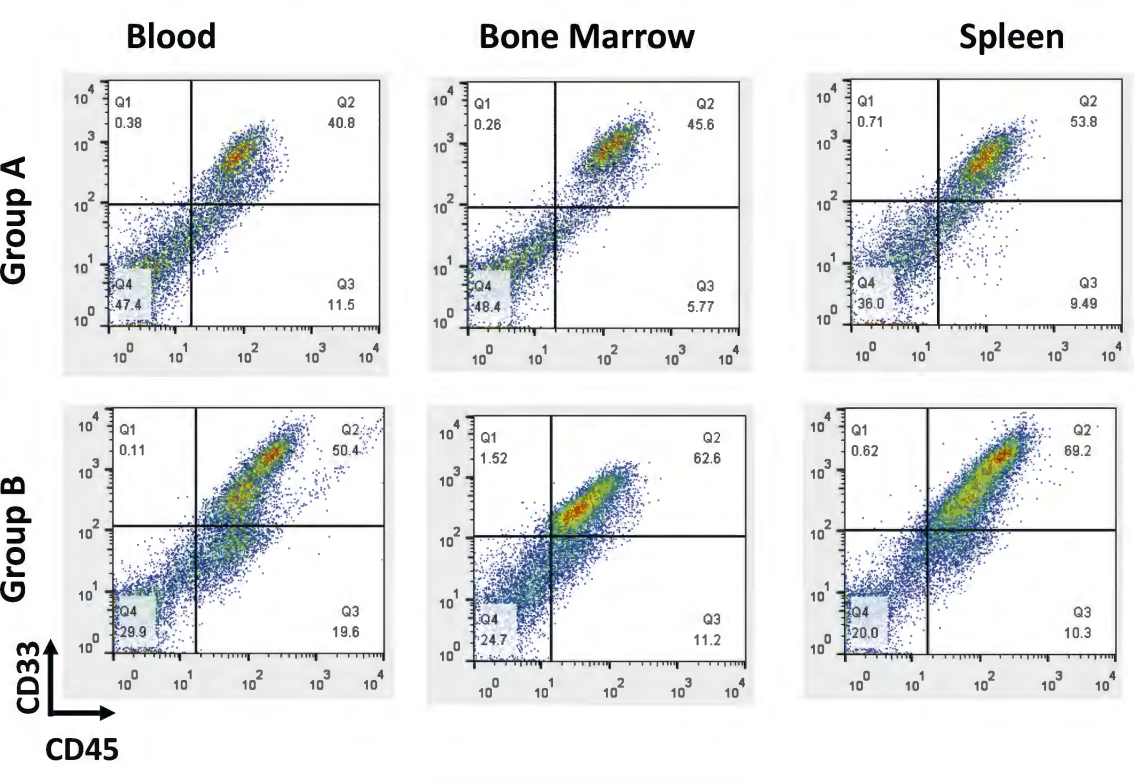
Blood
Bone Marrow
Spleen
Group A
Group B
Q1
0.38
Q2
40.8
Q4
47.4
Q3
11.5
Q1
0.26
Q2
45.6
Q4
48.4
Q3
5.77
Q1
0.71
Q2
53.8
Q4
36.0
Q3
9.49
Q1
0.11
Q2
50.4
Q4
29.9
Q3
19.6
Q1
1.52
Q2
62.6
Q4
24.7
Q3
11.2
Q1
0.62
Q2
69.2
Q4
20.0
Q3
10.3
CD33
CD45

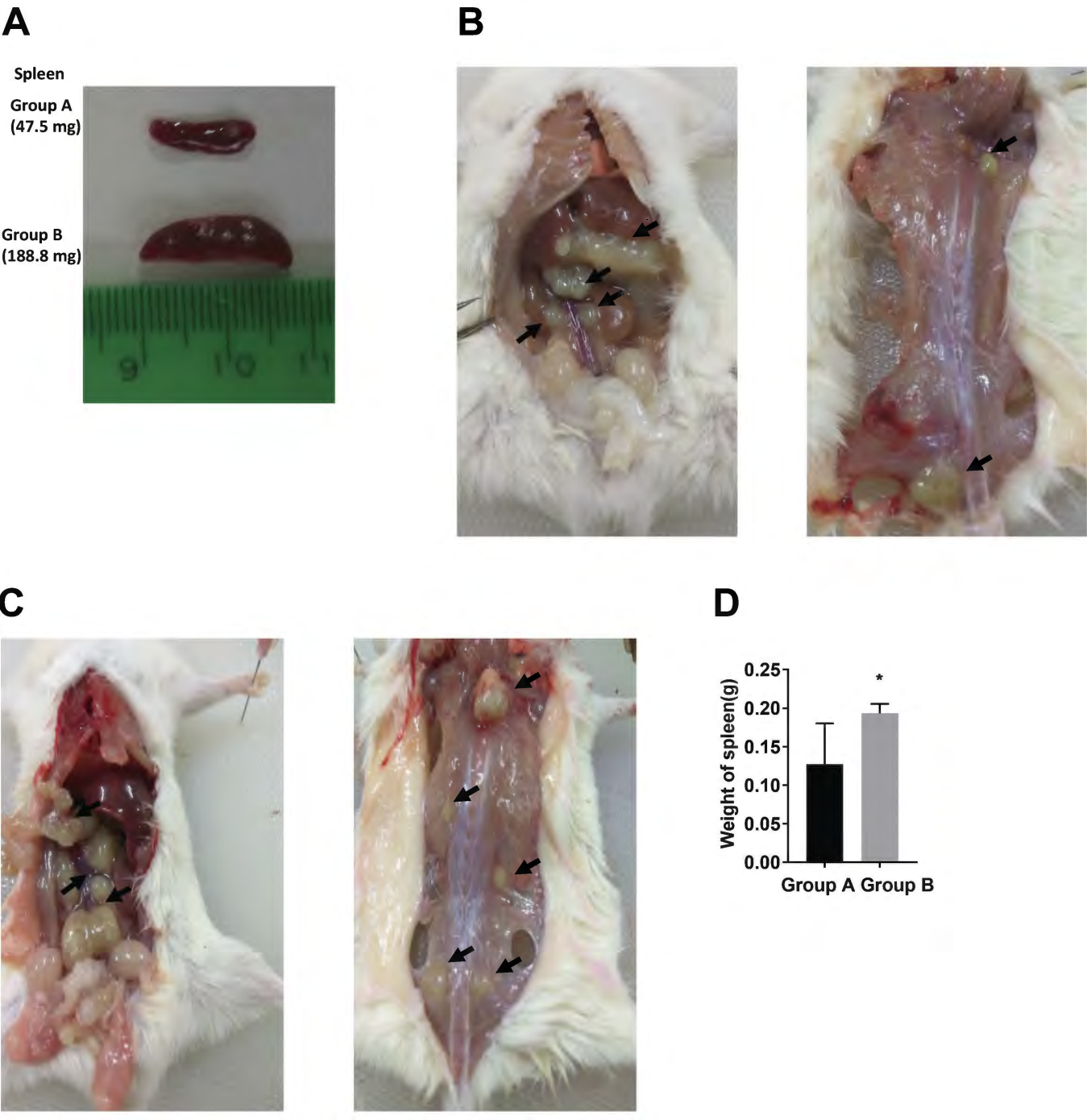
A
Spleen
Group A
(47.5 mg)
Group B
(188.8 mg)
B
C
D
Weight of spleen(g)
0.25
0.20
0.15
0.10
0.05
0.00
*
Group A Group B

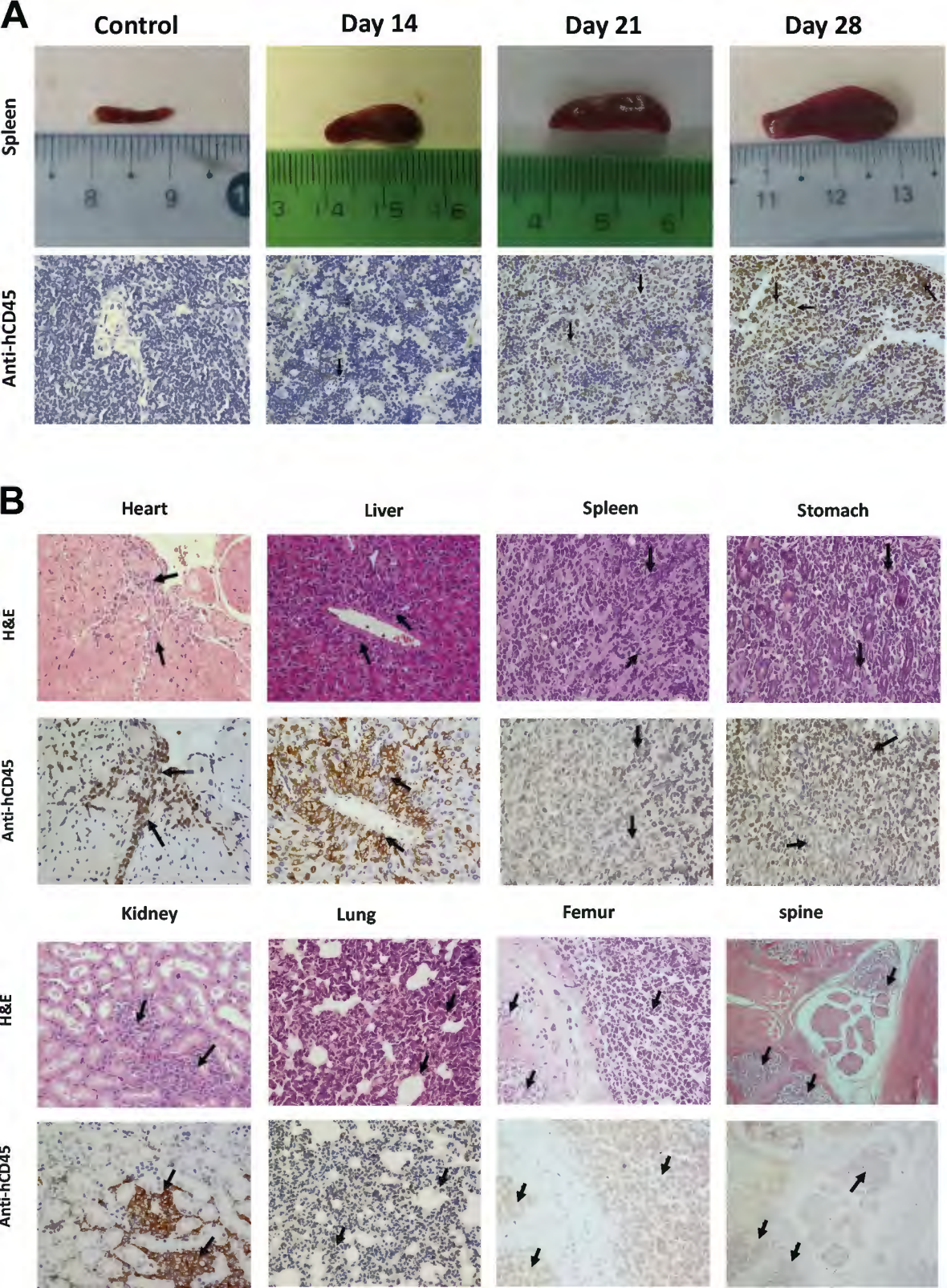
A
Control
Day 14
Day 21
Day 28
Spleen
Anti-hCD45
B
Heart
Liver
Spleen
Stomach
H&E
Anti-hCD45
Kidney
Lung
Femur
spine
H&E
Anti-hCD45